Model-free sliding-mode-based detection and estimation of backlash in drives with single encoder

Michael Ruderman and Leonid Fridman

***Abstract*—Backlash is a frequently encountered problem for various drives, especially those equipped with a single encoder onside of the controlled actuator. This paper proposes a sliding-mode differentiator-based estimation of unknown backlash size, while measuring the actuator displacement only. Neither actuator nor load dynamics are explicitly known, while a principal second-order actuator behavior is assumed. We make use of the different perturbation dynamics distinctive for different backlash modes and an unbounded impulse-type perturbation at impact. The latter leads to transient lost of the sliding-mode and allows for detecting an isolated time instant of the backlash occurrence. The proposed method is simple and unsensitive to residual system dynamics. The approach is experimentally evaluated on the data collected from a two-inertia-system with backlash in the coupling.**

***Index Terms*—sliding-mode observer, backlash, super-twisting algorithm, estimation, mechanical play, nonlinearities**

I. INTRODUCTION

For estimating unavailable states of dynamic systems, the sliding-mode observers, see e.g. [1], are particularly interesting since featuring the finite-time convergence [2]–[4] and robustness against the bounded matched perturbations. That means the estimated dynamic states can be used in an application (instead of the real quantities) after a finite-time, that starting from some initial conditions and independently of the time constants of the system dynamics under consideration. The backlash phenomenon in mechanical systems [5] constitutes a demanding case, where the unavailable state(s) and/or parameter(s) of a mechanical play need to be known either for the system control or monitoring purposes. Once the backlash size correspondingly state are known, these can be used in control, therefore reducing the undesirable lost motion own to the play and attenuating the impact and thus reducing wear and aging effects in mechanical drives with backlash; examples can be found in [5]–[9]. One should notice that the analysis of backlash disturbances in control engineering is not new, and the effects of backlash on the stability of closed-loops have been already addressed at a very early stage [10].

The sliding-mode-based approaches have been also shown for systems with backlash, considering the velocity observation [11] and switched twisting control [7]. However, the sliding-mode-based observation [11] requires both sides of the backlash system, to say motor and load, to be equipped with encoders for the relative displacement measurement. The largest part of mechanical systems with backlash are yet equipped with one-side sensing of displacement only, so that reliable backlash estimation constitutes a significant and challenging task desirable for various applications. Examples can be found in the motor drives [6], [12], vehicle steering and powertrain systems [13], [14], and others [15], [16]. It is also worth noting that the nonlinear, and even fractional-order, dynamics of systems with backlash has been addressed in [17], and as hybrid piecewise affine dynamics in [8], [9]. An approach for backlash identification, using a relay feedback velocity control loop, has been recently proposed in [18]. This requires, however, a high-precision motor encoder and can reveal sensitive to uncertain systems with a limited knowledge of system parameters and lower sampling, correspondingly quantization, characteristics of the feedback control. Another recent approach for robust backlash estimation in industrial drive-train systems can be found in [19], which relies on the sliding-mode perturbation observation and adaptive estimation principles. However, the approach requires a full vector of the motion system states, i.e. of motor and load, to be available.

The challenges with one-side backlash identification or online estimation, depending on the application requirements, are often due to uncertain parameters of the modeled motion dynamics and disturbing factors that cannot be taken into account when designing an estimation algorithm. Examples for that are the unknown and varying loads, uncertain damping across and inside of mechanisms containing backlash, sticking and drifting by-effects, and temporal propagation of crack effects and wear. Due to robustness, in regard to the system uncertainties, a sliding-mode-based approach for backlash estimation appears promising, especially when taking into account a variable structure feedback dynamics of the backlash load. Yet, to the best of our knowledge, neither of previous works made use of the mode-switching backlash behavior and its impact on the sliding-mode estimation errors.

This paper introduces a sliding-mode differentiator-based approach for detecting backlash and estimating its size in the drive systems, by using the position feedback of the actuated motor only. We use the fact of zero-converged error of position estimate at steady-state and discontinuous loss of sliding-mode upon backlash impact. From the associated and isolated time instants of the sliding-mode error we identify the backlash size within available motor displacement time-series. In what follows, the system dynamics is addressed in section II in context of system perturbations associated with backlash and unknown load dynamics. The second-order sliding mode STA algorithm is also briefly summarized for completeness. In section III, the backlash detection and estimation approach is explained in details, alongside with an application example. Evaluation on the experimental data from a two-inertia motor

M. Ruderman is with University of Agder, 4879-Grimstad, Norway. E-mail: michael.ruderman@uia.no

L. Fridman is with Universidad Nacional Autonoma de Mexico, 04510 Mexico City, CDMX, Mexico. Email: lfridman@unam.mx

setup with backlash in the geared coupling is provided in section IV. Finally, the conclusions are drawn in section V.

II. SYSTEM DYNAMICS WITH BACKLASH

A. Backlash perturbed second-order system

We consider a general class of the motion systems, driven by an actuator (further as motor), for which a stiff connection to load contains backlash. Having no explicit knowledge about drive-chain of the load, a principle structure of a two-inertia system with backlash, as shown in Fig. 1, can be assumed. The total unknown backlash size (denoted also as backlash gap) is 2β. The first inertial body is actuated by a generalized force u, which is an available system input. Both connected bodies are on the common ground with normal contact interfaces that induce counteracting forces, generally known as uncertain friction, see e.g. [20]. Note that independently whether a translational or rotational motion is in place, the generalized coordinates x_1 and x_2 of both rigid bodies with the total masses (inertias) m_1 and m_2 can be considered. Since our approach is model-free, neither load mass nor friction parameters (correspondingly models), are required to be explicitly known. While

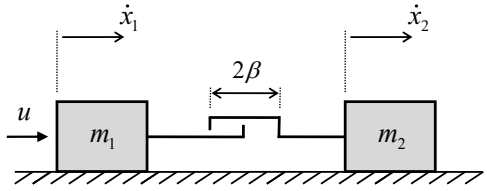

Fig. 1. Structure of two-inertia system with backlash

the motor and load dynamics are unknown, a principal second-order motor behavior in general form $f(t,x_1,w_1,u)$ can be assumed. The resulted system dynamics is then written as

$$\begin{aligned} \dot{x}_1 &= w_1, \\ \dot{w}_1 &= f(t,x_1,w_1,u)+\xi(t), \\ y &= x_1, \end{aligned} \tag{1}$$

where y is the single measured output state. The given input force u is assumed to be not affected by any process or measurement noise and is rather computational onside of an overlaying control system. The entire system uncertainties, correspondingly perturbations, are captured by $\xi(\cdot)$.

With respect to the system has backlash in the drive-chain (cf. Fig. 1) different operation modes appear depending on the backlash state $x_1 - x_2$. During the so-called *engagement* mode, i.e. when both backlash sides are in contact, it is valid $\dot{x}_2 \equiv \dot{x}_1 = w_1$. At the same time, nothing exact can be said about $\dot{x}_2$ within a *gap* mode, i.e. when the motor and load are decoupled from each other. During the *impact*, with the corresponding changes of momentum $\gamma = m_1\dot{x}_1$, the motor dynamics is subject to an impulse-type excitation, cf. [21]. Without an explicit knowledge of the load dynamics one can write for the backlash perturbation

$$\xi = \begin{cases} \alpha\dot{w}_1 + g_1(t) + g_2(t) & \text{in engagement mode,} \\ g_1(t) & \text{in gap mode,} \\ \dot{\gamma} & \text{at impact,} \end{cases} \tag{2}$$

cf. with backlash modeling introduced in [18]. The functions $g_1(\cdot)$ and $g_2(\cdot)$ are associated with unknown parts of the motor and load dynamics, correspondingly. The negative constant of the mass ratio is denoted by $\alpha = -m_2/m_1$ with $-\infty < \alpha < 0$. Note that depending on the motor and load dimensions $\alpha \in (-10, -0.1)$ can be assumed in the most of application cases, while some nominal gear ratio is already included.

From (2) it turns out that an upper boundary for the backlash perturbations can be found, correspondingly approximated, for a given system, except the impact transitions at which the momentum experiences discontinuously. For showing this, consider an ideal elastic impact of two colliding masses, i.e. with unity restitution coefficient, which is yet valid in case of minor plastic deformations. We note that an, otherwise, non-negligible plastic impact is something rather unusual for constructive elements containing backlash. Even though $\dot{x}_2$ is generally not given before and during the backlash impact, the changes of $\dot{x}_1$, and therefore γ, can be directly assessed from

$$\dot{x}_1^+ = \frac{\dot{x}_1(1+\alpha) - 2\alpha\dot{x}_2}{1-\alpha}, \tag{3}$$

which follows from the Newtons law for unity restitution coefficient. Here $\dot{x}_1^+$ denotes the motor velocity immediately after the backlash impact. It is evident that, except the case $\dot{x}_1 = \dot{x}_2 = 0$, the motor velocity will always experience a step-wise change, leading to an impulsive excitation by perturbation term. This allows considering the perturbation term, further denoted with subscript index i for 'impact', as a weighted Dirac (delta) impulse, cf. with [18],

$$\xi_i = W m_1 \delta(t - t_i), \tag{4}$$

while a relative impulse weight $-\infty < W < \infty$ remains uncertain, due to uncertainties in (3). Here we should also recall that the delta function $\delta(t-t_i)$ is defined, in terms of distribution theory, at t_i only and is zero elsewhere. Yet delta is satisfying the identity property of integration over the argument

$$\int \delta(z)dz = 1.$$

It is evident that no upper bound can be given for (4), the matter of fact which brings us in the position to derive an approach of detecting and identifying backlash by using the second-order sliding mode.

B. Second-order sliding mode differentiator

For observation of the motor states, i.e. x_1 and w_1, we are using the second-order sliding-mode super-twisting algorithm (STA) [22]. Here we stress that if a model of the nominal system dynamics is available, an explicit second-order sliding-mode observer [1] can be used for faster convergence and robust state estimation while applying lower feedback gains. In

this work we, however, refrain from an explicit system knowledge and assume general lack of the identified parameters, thus relying solely on a STA-based differentiator [23].

The second-order sliding-mode differentiator takes the form

$$\dot{\hat{x}}_1 = \hat{w}_1 + k_1 |y - \hat{x}_1|^{1/2} \text{sign}(x_1 - \hat{x}_1), \quad (5)$$

$$\dot{\hat{w}}_1 = k_2 \, \text{sign}(y - \hat{x}_1), \quad (6)$$

where the estimator gains can be assigned as $k_2 = 1.1L$ and $k_1 = 2.028\sqrt{k_2}$, according to the methodology [24] that has been also recently confirmed in an experimental study [25]. Note that the second-order upper bound $\ddot{y} \leq L$ of an uncertain system dynamics is generally not given, so that L is the single design parameter we address in the following for various perturbation modes of (1). Here one should recall that for an appropriate k_1, k_2 selection and an upper bounded dynamics perturbation, i.e. $L \geq |f + \xi|$, the STA ensures the equalities $(y - \hat{x}_1) = (\dot{y} - \hat{w}_1) = 0$ hold after finite-time transients. Further we note that the convergence time of a STA-based estimate can be explicitly determined, e.g. as proposed in [4], for the given initial values of the state estimation errors. However, we are not making use from the convergence time values since the initial values remain unavailable in our case. At the same time, we use a fact that for $L << |\xi|$, where L appears as a boundness constant for STA parameterization, the second-order sliding-mode is lost. In this regard, an unbounded impulse-type perturbation produces discontinuity in trajectory of the estimation error as addressed below.

III. BACKLASH DETECTION AND ESTIMATION

A. Estimation error dynamics

Introducing the state estimation errors $e_x = x_1 - \hat{x}_1$ and $e_w = w_1 - \hat{w}_1$ and substituting (1) into (5), (6) one obtains the estimation error dynamics as

$$\dot{e}_x + k_1 |e_x|^{1/2} \, \text{sign}(e_x) = e_w, \quad (7)$$

correspondingly

$$\dot{e}_w = f + \xi - k_2 \, \text{sign}(e_x). \quad (8)$$

It is evident that the left-hand side of (7) describes a stable first-order dynamics, provided $k_1 > 0$, so that $e_x \to 0$ for $e_w \to 0$. It is also worth noting that for a steady-state motion, i.e. $f = 0$, the e_w dynamics is excited once by the system perturbation and once by an alternating (chattering) sign of the e_x value. Recall that the finite-time stability of an unperturbed case, i.e. $\xi = 0$, follows directly from the strict Lyapunov function candidate derived for STA according to [3]. Following to that, the stability of $(e_x, e_w) = \mathbf{0}$ equilibrium is entirely determined by stability of the gains matrix [3]

$$A = \begin{pmatrix} -0.5k_1 & 0.5 \\ -k_2 & 0 \end{pmatrix},$$

which is the estimator design parameter.

For the perturbed case, more precisely partially-perturbed since ξ affects only (8) but not (7), the STA requires that $|f + \xi| \leq L$ holds, see [3] and related references therein. That means the perturbation term has to be globally bounded by $L - |f|$, which appears as a design parameter dependent on the system dynamics (1), (2). From (2), (4) on can recognize that the upper bound can be determined for the engagement and gap modes of backlash, but not for the impact mode of one-way transitions between both. An unbounded impulse-type perturbation occurs during the backlash impact, therefore representing a short-term transient excitation of (8) and step-wise excitation of (7) correspondingly. Following to that, an apparent peaking in the e_x-trajectories is expected, allowing for backlash detection and identification, and that for a relatively arbitrary periodic motion with an amplitude $> 2\beta$.

B. Upper bound of dynamics perturbation

For having estimate on the upper bound of L, consider first the nominal motor dynamics and that for an unperturbed case, i.e. $\xi = 0$. In the most simple case, the nominal motor dynamics can be captured by

$$f = -d_1/m_1 \, w_1 + K_m/m_1 \, u, \quad (9)$$

where the linear motor damping is denoted by d_1 and the motor torque constant by K_m correspondingly. Assuming the inherent actuator saturations i.e. $|u| \leq U_{\max}$, and capturing the input-output motor behavior by an associated transfer function $w_1(s)/u(s) = K_m(m_1 s - d_1)^{-1}$, with s to be the Laplace variable, one can easily obtain

$$|f| = \frac{U_{\max}}{m_1} \left(K_m - K_m \frac{d_1}{m_1 s + d_1} \right). \quad (10)$$

From (10) it becomes evident that the maximal amplitude of f appears at $s \to \infty$, meaning a high-frequent motor actuation. On the contrary, for $s \to 0$, meaning a steady-state or very low-frequent input excitation, $|f| \to 0$. The above implies

$$|f| \leq \frac{U_{\max} K_m}{m_1}. \quad (11)$$

Here it is worth of recalling that (11) remains valid independently of the instantaneous backlash mode.

Now consider the first two backlash modes, i.e. engagement and gap, while for the impact mode a perturbation is unbounded according to (4). It can be recognized from (2) that during the engagement mode a perturbation amplitude is larger than within the gap mode – not surprisingly since both the motor and load motion systems become coupled. Further it is apparent that (11), modified in the denominator by $m_1 + m_2$ instead of m_1, represents a maximal possible acceleration of the actuated motion when the motor and load are coupled. For both unknown dynamic functions, cf. (2), assume an upper bound so that $|g_1|, |g_2| \leq G m_1^{-1}$ and that for some constant $G > 0$. Note that G has physical dimension of a force and, therefore, can be considered as a design parameter available for the given mechanical system. Substituting the above assumptions into (2), and that for engagement mode further indicated by the subscript index e, one can obtain

$$|f + \xi_e| \leq \frac{|\alpha| U_{\max} K_m + (1 - \alpha)(U_{\max} K_m + 2G)}{m_1 (1 - \alpha)}. \quad (12)$$

The inequality determines an upper bound L for the entire motion dynamics, except the backlash impact at which it

undergoes an impulse-type discontinuity. It is worth emphasizing that while $U_{\max}$, K_m, and m_1 can be assumed as the known system parameters – all related to the motor drive – the α and G constants give solely the boundness conditions for an external load system. For making the engagement and gap modes well-distinguishable, and that from a sliding-mode estimation point of view, it is suggested to assign

$$\frac{U_{\max}K_m+G}{m_1} < L < \frac{|\alpha|U_{\max}K_m+(1-\alpha)(U_{\max}K_m+2G)}{m_1(1-\alpha)}. \tag{13}$$

Consequently, the second-order sliding mode should converge within the gap, provided the system remains there sufficiently long, and becomes continuously excited, correspondingly diverges from zero estimation error, during the engagement mode. During impact transitions between both, the $e_x(t)$ error state undergoes a distinctive peaking, and that independently of the upper bound assignment (13). In real applications, where 2β is significantly smaller comparing to x_1 and x_2 displacements, a zero convergence of sliding-mode within the backlash gap can be hardly expected. The latter will be, namely, passed through relatively quickly, i.e. before the finite-time convergence of the sliding-mode. Nevertheless, a varying pattern of $e_x(t)$ trajectory distinctive between the backlash modes and containing the impact-related peaking allows for estimating the backlash sizes as shown below for applications.

C. Estimation procedure

For systems with backlash satisfying the above assumptions about dynamics and upper bounds, the estimation of backlash size can be performed by the sequence of following steps (S).

- S1: Fed the motor with $u(t) = U\sin(\omega t)$, with $U < U_{\max}$ yet sufficient for inducing a periodic motion, and $\omega^{-1} \gg$ *time constant* of the system (9);
- S2: Monitor the estimation error e_x, amplified by factor N for x_1 and e_x are on a comparable scale, after zero convergence, i.e. $e_x \approx 0$ with respect to noise;
- S3: Detect divergence of $e_x(t)$ and set $t_1 = t$;
- S4: Detect backlash impact by an abrupt reversal of $e_x(t)$ and set $t_2 = t$;
- S5: From the measured motor position, compute the backlash size by $2\hat{\beta} = |x_1(t_2) - x_1(t_1)|$;
- S6: To increase generalizability of the estimate, average $2\hat{\beta}$ by repeating S1-S5 over multiple periods.

D. Application example

A two-inertia system, cf. Fig. 1, is modeled as (1), (9), while the backlash is described by means of a most simple dead-zone-based approach [9], cf. with [5]. The assumed motor parameters are $U_{\max}$=0.5, K_m=0.172, m_1=8.78e–4, β=9.4e–3. Note that the parameter values are approaching the identified experimental system whose measured data are further used for experimental evaluation in Section IV. The assigned motor damping is d_1=6.2e–2 while an additional torsional (i.e. structural) damping is also assumed when modeling backlash. For more details on the backlash modeling used for the simulation we refer to [9]. For the load boundness conditions, the values α=–1 and G = 5e–5 are assumed, while the latter results from $g_2(t) = -0.035\dot{x}_2 - 0.05\text{sign}(\dot{x}_2)$ which is taken for numerical simulation of the load side. No additional motor-side perturbations, meaning $g_1 = 0$, are assumed for the sake of simplicity. At the same time, it is worth noting that g_2 contains a sign-dependent term that approximates nonlinear Coulomb friction with discontinuity at zero crossing. The assumed numerical values, substituted into (13), results in

$$98 < L < 147.$$

Following to that $L = 100$ is assigned as the design parameter for determining the corresponding STA gains.

The sinusoid motor input $u(t) = 0.5\sin(0.1 \cdot 2\pi \cdot t)$ is applied, and the resulted motor output displacement $x_1(t)$, both depicted in Fig. 2 (a), is used as the single measurement for STA-based backlash detection and identification described above. Despite the motor displacement discloses certain distor-

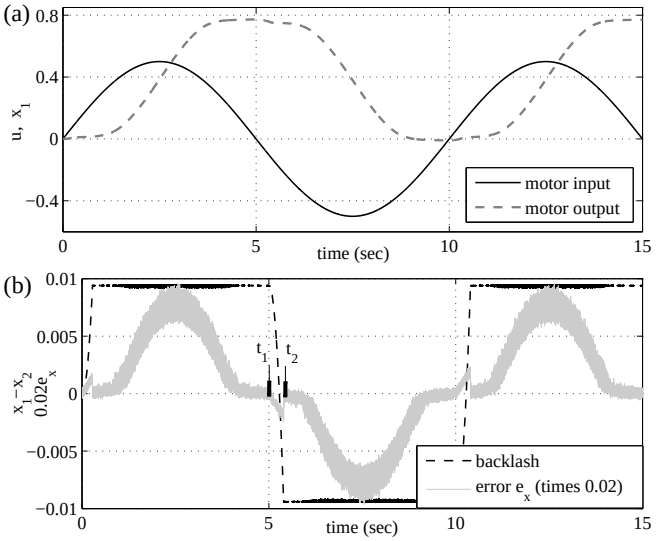

Fig. 2. Motor input u versus motor output displacement x_1 in (a), backlash state $x_1 - x_2$ versus state estimation error e_x in (b)

tions at the second half of the peaks (around time $t = 5$ and $t = 10$ sec), which can be associated with backlash perturbations, no direct delectability appears possible when analyzing $x_1(t)$ time series. Also we note that the shown motion trajectory is under ideal numerical simulation conditions, while real measurements can be additionally affected by noise. In Fig. 2 (b), the dynamic backlash state $(x_1 - x_2)(t)$ is shown, for the sake of comprehensibility, versus the state estimation error $e_x(t)$. The latter is scaled down by the factor $\times 0.02$ for making both signals comparatively visible. One can see that close to a motion reversal and low-level input excitation, meaning some steady-state conditions, the state estimation error converges to zero. Starting from the time instant t_1, labeled in Fig. 2 (b), the $e_x(t)$ value starts rapidly decreasing, i.e. diverging from zero, as implication of a discrete change of the backlash mode. At the time instant t_2, the $e_x(t)$ value undergoes a stepwise change which is well-detectable as labeled in Fig. 2 (b). This occurs during the backlash impact as has been analyzed above, cf. Section III-A. Note that the labeled t_1 and t_2 time instants

coincide quite accurately with the backlash gap mode, i.e. $|x_1(t)-x_2(t)|<2\beta$, cf. with the backlash state depicted in Fig. 2 (b). While a stepwise discontinuity in the $e_x(t)$ trajectory serves for detecting a backlash in the system, the estimated gap size reads off directly as

$$2\hat{\beta} = |x_1(t_2)-x_1(t_1)|.$$

IV. EXPERIMENTAL EVALUATION

A. Two-inertia system with backlash

Real-time experimental data we are using for practical evaluation of our approach are recorded on a laboratory setup consisting of two identical motors, with a 20-bit high-resolution encoder each. The first one is low-level torque controlled and denoted further as *motor*. The second one serves as a passive rotary *load*. Note that solely the measured angular displacement of the (first) motor is used by our approach, and the available load encoder serves for the sake of reference measurements only. The utilized geared coupling between the motor and load contains backlash. For more technical details on the laboratory experimental we refer to [9], [18]. The input-output backlash map has been measured, for the sake of reference reference, with both encoders as shown in Fig. 3. Note that due to an input excitation (applied to the current- correspondingly torque-control) with 1 Hz frequency, the recorded backlash trajectories are not entirely static and contain certain transients during the impact. Furthermore, it should be underlined that the trajectories going in positive direction are not entirely symmetrical to those in negative direction. They diverge from a poorly kinematical backlash, i.e. ideal play-type hysteresis map, due to additional adhesive by-effects in the geared coupling. Nevertheless, an unambiguous backlash gap of about $2\beta = 0.019$ rad can be read off and assumed as a reference value.

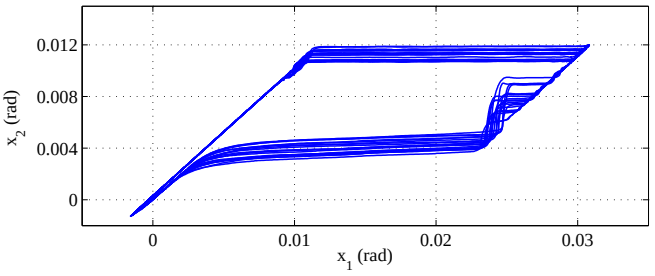

Fig. 3. Backlash measured by means of motor- and load-side encoder

B. Identification of backlash gap

The experimental backlash identification is performed following the methodology provided in Section III-C. A periodic torque excitation with 1 Hz frequency and 0.1 Nm amplitude has been applied to the two-inertia system with backlash. The measured backlash response is shown versus the input torque in Fig. 4. One can recognize a periodic backlash pattern, while the forward gap transitions are lagged behind the input torque zero-crossings. Note that a relatively small motor displacement, close to the backlash gap size (cf. with Fig. 5 is purposefully induced for a better visualization. The larger displacement amplitudes are equally applicable without changing identification methodology. It is also worth noting that a low displacement constitutes rather a 'worst case' scenario, since the sliding-mode has less time for e_x convergence to zero.

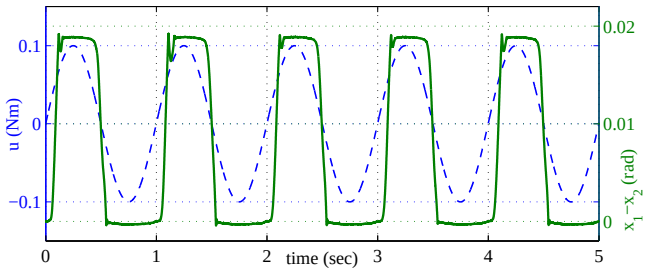

Fig. 4. Measured backlash state versus periodic torque excitation

The state estimation error e_x, multiplied with factor 50 for a better visualization, is shown opposite to the measured motor displacement in Fig. 5. One can recognize a sufficiently uniform periodic pattern of $e_x(t)$, so that an arbitrarily picked-out period can be used for signal analysis and identification of the backlash gap size. The bound value $L = 40$ has been

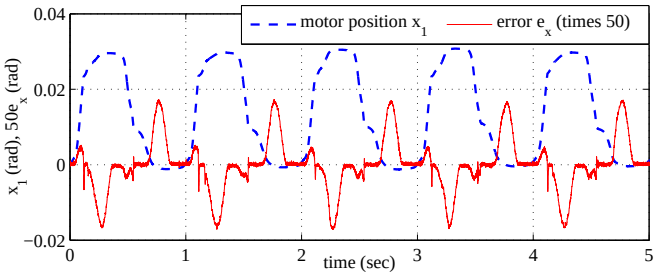

Fig. 5. Measured motor displacement $x_1(t)$ versus state estimation error $e_x(t)$, multiplied by factor 50 for the sake of a better visualization

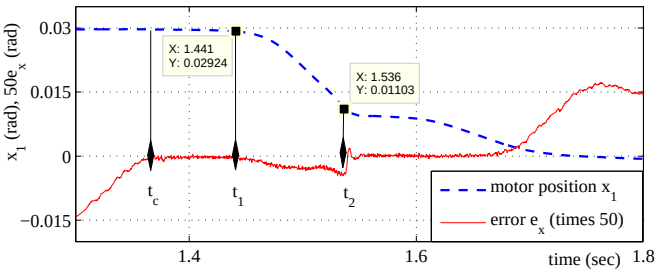

Fig. 6. Zoom-in of the measured motor position (x_1) and estimation error ($50 \times e_x$) for analysis and detection of the backlash gap

assigned based on pre-knowledge of the system parameters, cf. [9], [18], and in order to deal with non-zero noise subject to amplification. Note that a higher L value, like one determined from the model parameters in Section III-C, is equally possible but will shortening the convergence time of $e_x(t)$ and enhancing ist chattering pattern. Both would imped an accurate isolation of t_1 and t_2 time instants.

A zoom-in of an arbitrary chosen period is shown in Fig. 6. One can recognize that at steady-state of the motor position,

i.e. before motion reversal, the $e_x(t)$ trajectory converges to zero, labeled by t_c. Afterwards, the observation error remains zero until an apparent motion direction changes, i.e. the motor 'decouples' from the load due to the backlash. Apparently, this structure-switching transition sufficiently excites $e_x(t)$ which, in turn, diverges from zero, cf. with Fig. 2. The corresponding time instant is labeled by t_1. As next, a stepwise excitation of the sliding-mode dynamics occurs due to the backlash impact, once losing the gap mode at the time t_2. One can see that, due to an apparently stiff impact, the transient error dynamics tends even to some minor oscillations, which are visible at time close to t_2 from the right. Following the procedure developed in Section III the backlash gap is identified as

$$2\hat{\beta} = |x_1(t_2) - x_1(t_1)| = 0.018\,rad.$$

The estimated value differs from the measured nominal one by about 5%, that is sufficiently accurate in regard to the limited system knowledge and single motor-side measurement. Auto-recording and averaging of $2\hat{\beta}$ over multiple periods can further improve the estimation accuracy.

V. CONCLUSIONS

This paper introduced a new approach for detecting and identifying the unknown backlash in the drive systems which are equipped with a single displacement sensor (encoder) placed on the controlled actuator. The method incorporates the second-order sliding-mode STA-based estimator. Neither explicit system model nor additional system measurements are required a priori. Only the second-order actuator dynamics and the basic motor parameters, like torque constant and limits, linear damping, and inertia, are assumed. Analyzing the load- and backlash-related perturbations, the state estimation error dynamics is derived, and the upper bound for the STA-based differentiator is determined as a design parameter for assignment of the STA gains. We demonstrated and formalized how the backlash gap size can be accurately identified from the time-series. Also an experimental evaluation, based on recorded real-time data from a motor-bench setup, is shown as efficient with the proposed identification method. Future works can be concerned with sensitivity analysis of the proposed method, in regard to lower sampling and quantization of the actuator signals and evaluation with other application cases.

ACKNOWLEDGMENT

This work has received funding from the European Union Horizon 2020 research and innovation programme H2020-MSCA-RISE-2016 under the grant agreement No 734832. The authors are grateful to Hori-Fujimoto Lab (University of Tokyo), especially Shota Yamada, for experimental data.

REFERENCES

[1] J. Davila, L. Fridman, and A. Levant, "Second-order sliding-mode observer for mechanical systems," *IEEE Transaction on Automatic Control*, vol. 50, no. 11, pp. 1785–1789, 2005.

[2] A. Polyakov and A. Poznyak, "Reaching time estimation for super-twisting second order sliding mode controller via lyapunov function designing," *IEEE Transactions on Automatic Control*, vol. 54, no. 8, pp. 1951–1955, 2009.

[3] J. A. Moreno and M. Osorio, "Strict Lyapunov functions for the super-twisting algorithm," *IEEE Transactions on Automatic Control*, vol. 57, no. 4, pp. 1035–1040, 2012.

[4] R. Seeber, M. Horn, and L. Fridman, "A novel method to estimate the reaching time of the super-twisting algorithm," *IEEE Transactions on Automatic Control*, vol. 63, no. 12, pp. 4301–4308, 2018.

[5] M. Nordin and P.-O. Gutman, "Controlling mechanical systems with backlash a survey," *Automatica*, vol. 38, no. 10, pp. 1633–1649, 2002.

[6] D. Gebler and J. Holtz, "Identification and compensation of gear backlash without output position sensor in high-precision servo systems," in *IEEE Annual Conference of Industrial Electronics Society (IECON'98)*, 1998, pp. 662–666.

[7] Y. Orlov, L. Aguilar, and J. Cadiou, "Switched chattering control vs. backlash/friction phenomena in electrical servo-motors," *International Journal of Control*, vol. 76, no. 9-10, pp. 959–967, 2003.

[8] P. Rostalski, T. Besselmann, M. Barić, F. V. Belzen, and M. Morari, "A hybrid approach to modelling, control and state estimation of mechanical systems with backlash," *International Journal of Control*, vol. 80, no. 11, pp. 1729–1740, 2007.

[9] S. Yamada, M. Ruderman, and H. Fujimoto, "Piecewise affine (PWA) modeling and switched damping control of two-inertia systems with backlash," in *IEEE International Workshop on Advanced Motion Control (AMC)*, 2018, pp. 479–484.

[10] A. Tustin, "The effects of backlash and of speed-dependent friction on the stability of closed-cycle control systems," *Journal of the Institution of Electrical Engineers - Part IIA: Automatic Regulators and Servo Mechanisms*, vol. 94, pp. 143–151, 1947.

[11] R. Merzouki, J. Davila, L. Fridman, and J. Cadiou, "Backlash phenomenon observation and identification in electromechanical system," *Control Engineering Practice*, vol. 15, no. 4, pp. 447–457, 2007.

[12] S. Villwock and M. Pacas, "Time-domain identification method for detecting mechanical backlash in electrical drives," *IEEE Transactions on Industrial Electronics*, vol. 56, no. 2, pp. 568–573, 2009.

[13] A. Lagerberg and B. Egardt, "Backlash estimation with application to automotive powertrains," *IEEE Transactions on Control Systems Technology*, vol. 15, no. 3, pp. 483–493, 2007.

[14] X. Huang and J. Wang, "Identification of ground vehicle steering system backlash," *Journal of Dynamic Systems, Measurement, and Control*, vol. 135, no. 1, p. 011014, 2013.

[15] J. W. Peine, V. Agrawal, and W. J. Peine, "Effect of backlash on surgical robotic task proficiency," in *IEEE 4th International Conference onBiomedical Robotics and Biomechatronics*, 2012, pp. 799–804.

[16] T. K. Morimoto, E. W. Hawkes, and A. M. Okamura, "Design of a compact actuation and control system for flexible medical robots," *IEEE Robotics and Automation Letters*, vol. 2, no. 3, pp. 1579–1585, 2017.

[17] R. S. Barbosa and J. T. Machado, "Describing function analysis of systems with impacts and backlash," *Nonlinear Dynamics*, vol. 29, no. 1, pp. 235–250, 2002.

[18] M. Ruderman, S. Yamada, and H. Fujimoto, "Backlash identification in two-mass systems by delayed relay feedback," *Journal of Dynamic Systems, Measurement, and Control*, vol. 141, no. 6, p. 061007, 2019.

[19] D. Papageorgiou, M. Blanke, H. H. Niemann, and J. H. Richter, "Robust backlash estimation for industrial drive-train systems–theory and validation," *IEEE Transactions on Control Systems Technology*, no. 99, pp. 1–15, 2018.

[20] M. Ruderman and M. Iwasaki, "Observer of nonlinear friction dynamics for motion control," *IEEE Transactions on Industrial Electronics*, vol. 62, no. 9, pp. 5941–5949, 2015.

[21] M. Ruderman, "Relay feedback systems - established approaches and new perspectives for application," *IEEJ Journal of Industry Applications*, vol. 8, no. 2, pp. 271–278, 2018.

[22] A. Levant, "Sliding order and sliding accuracy in sliding mode control," *International Journal of Control*, vol. 58, no. 6, pp. 1247–1263, 1993.

[23] A. Levant, "Robust exact differentiation via sliding mode technique," *Automatica*, vol. 34, no. 3, pp. 379–384, 1998.

[24] U. P. Ventura and L. Fridman, "Design of super-twisting control gains: a describing function based methodology," *Automatica*, vol. 99, pp. 175–180, 2019.

[25] M. Ruderman and L. Fridman, "Use of second-order sliding mode observer for low-accuracy sensing in hydraulic machines," in *IEEE International Workshop on Variable Structure Systems and Sliding Mode Control (VSS18)*, 2018, pp. 315–318.